J. Chem. Soc., Faraday Trans. 1, 1988, **84**(5), 1639–1651

Raman Spectra of Potassium *trans*-4-Hexenoate and Conformational Change on Micellization

Hirofumi Okabayashi,* Koji Tsukamoto, Kunihiro Ohshima and Keijiro Taga
Department of Applied Chemistry, Nagoya Institute of Technology, Gokisocho, Showa-ku, Nagoya 466, Japan

Etsuo Nishio
Perkin-Elmer Japan, Osaka Laboratory, Miyahara, Yodogawaku, Osaka, Japan

The infrared and Raman spectra of potassium *trans*-4-hexenoate (PT4H) have been measured in the crystalline state and in aqueous solution. Normal coordinate calculations have been carried out to explain the vibrational spectra. For crystalline PT4H it is concluded from the vibrational spectra in the 700–100 cm^{-1} region that the *trans*–skew (TS) and *trans–cis* (TC) forms coexist at 300 K and the TS form is stabilized at 100 K. For the PT4H ions in aqueous solution the TS form was found to be predominantly stabilized on micellization. In particular, the Raman spectra of a PT4H–H_2O solution in the 1700–700 cm^{-1} range were investigated at various concentrations, and it was found that the stabilization of the TS form is reflected in vibrational modes characteristic of the —CH=CH— and CH_2 groups. The difference Fourier-transform infrared (F.t.i.r.) spectra of PT4H–H_2O (or PT4H–D_2O) solutions have also been measured at various concentrations. The infrared absorption spectra of water were successfully cancelled out in the 1500–900 cm^{-1} region for H_2O and in the 1700–1300 and 1000–700 cm^{-1} regions for D_2O. The concentration dependence of the difference F.t.i.r. spectrum was used to investigate conformational changes upon micellization.

Vibrational spectroscopy has been extensively used in studying the structural ordering of the saturated-hydrocarbon parts of fatty acids and their salts and phospholipids. In particular, Raman scattering has played an important role in conformational studies of surfactants.[1–6] The effect of an unsaturated acyl chain on the physical properties of a phospholipid bilayer has been studied in relation to the functions of biological membranes.[7–9] Raman scattering has also been used to study structural ordering and in carrying out conformational studies of bilayers and micelles having unsaturated chains.[10–15]

The utility of the vibrational spectrum in the 1200–1000 cm^{-1} region for investigating the conformation of unsaturated fatty acids has been pointed out by Lippert and Peticolas.[10] Okabayashi *et al.* have shown from Raman studies in the 1200–200 cm^{-1} region that a specific rotational isomer of simple unsaturated surfactants is preferentially stabilized on aggregation.[14,15]

In recent years, Fourier transform infrared (F.t.i.r.) spectroscopy has permitted precise studies of molecular and conformational properties, and has made it possible to study aqueous micellar solution,[16,17] multibilayer lipid membranes[18–23] and monomolecular films.[24]

In the present work, Raman scattering and the F.t.i.r. technique have been used to investigate the conformational changes of simple unsaturated surfactants upon micellization.

Experimental

Materials

trans-4-Hexenoic acid was synthesized from crotyl bromide and dimethylmalonate, following the method of Eccot and Linstead[25] (boiling point of *trans*-4-hexenoic acid, 106 °C at 17 mmHg†). Identification of the sample was made from ^{1}H and ^{13}C n.m.r. spectra. Potassium *trans*-4-hexenoate (PT4H) was prepared from the corresponding acid and potassium hydroxide in methanol and was recrystallized in the same solvent.

Infrared Absorption Spectra Measurements

The infrared absorption spectra were recorded with a JASCO-DS-402G double-beam grating spectrometer in the 4000–400 cm^{-1} range and with a Hitachi FIS-3 double-beam grating spectrometer in the 400–30 cm^{-1} region.

Fourier-transform Infrared Spectra Measurements

Fourier-transform infrared (F.t.i.r.) spectra were measured with a Perkin-Elmer 1700 Fourier-transform infrared spectrometer. An attenuated total reflection (ATR) instrument (ZnSe, sample volume 350 mm^3) was used for measurements on the aqueous solutions.

Raman Scattering Measurements

Raman spectra were measured with a JEOL model 400D Raman spectrometer. The 514.5 nm line of an argon-ion laser (NEC GLS-3200, 2W) was used as an excitation source.

Normal-coordinate Treatment

A normal-coordinate analysis of the PT4H ion was made for possible rotational isomers; *trans*–skew (TS), *trans–cis* (TC), *gauche*–skew (GS), *gauche'*–skew (G'S) and *gauche–cis* (GC), the order going from the CO_2^- group to the terminal group. The other isomers, which were omitted from the calculations, are expected to be much less stable owing to steric hindrance.

In the normal-coordinate calculations we assume that the infrared absorption bands increased in intensity on cooling, and the corresponding Raman bands arise from the TS form. This assumption is reasonable by reference to the infrared and Raman studies of potassium 5-hexenoate and potassium 4-pentenoate,[15] Raman studies of various long-chain unsaturated fatty acids[26] and X-ray diffraction analysis of oleic acid.[27]

The Urey–Bradley–Shimanouchi force field (UBSFF) was used for calculations of normal mode frequencies. The calculations contain the force constants for (*a*) the *cis*-C···C repulsion and (*b*) the interaction between =CH— out-of-plane wagging and C=C torsional modes. Force constants of alkenes and potassium carboxylates were initially used, and those used in the molecular skeleton calculations were modified to obtain the best fit between the observed wavenumbers of the crystalline PT4H and those calculated by a least-squares method. The modified force constants (table 1) were used for calculations on other isomers.

A Melcom-Cosmo 700III/MP computer was used for all calculations by using the program NCTB prepared by Shimanouchi *et al.*[28]

† 1 mmHg = 1.3322×10^2 Pa.

Table 1. Force constants and structural parameters for PT4H[a]

force constant	value	force constant	value
K(C—H), CH_3	4.28	F(C′—C—H)	0.38
K(C—H), CH_2	4.09	F(C=C—C)	0.40
K(C—C)	2.60	F(C—C′—H)	0.51
K(=C—C)	3.25	F(C=C—H)	0.45
K(C=C)	7.55	F(C—C—O)	1.22
K(=CH)	4.39	F(O—C—O)	1.20
K(C—CO)	2.94	F(C—C—C)	0.40
K(C—O)	7.35	W(=CH)	0.32
H(C—C—H)	0.243	W(CO_2)	0.62
H(H—C—H)	0.35	Y(—C—C)	0.08
H(=C—C—C)	0.25	Y(=C—C)	0.085
H(C′—C—H)	0.22	Y(C=C)	0.47
H(C=C—C)	0.31	WW(H···H)	−0.044
H(C—C′—H)	0.16	WY(HC=C)	0.025
H(C=C—H)	0.21	R(—C—C=), C*=CCC*	0.33
H(C—C—O)	0.14	TC(H—H)	0.096
H(O—C—O)	0.65	GC(H—H)	−0.036
H(C—C—C)	0.12	P(CO_2)	0.10
F(C—C—H)	0.40	P(CH_2)	−0.10
F(H—C—H)	0.21	P(CH_3)	−0.06
F(=C—C—C)	0.40		

bond length, r (a.u.)

r(C=C): 1.335, r(=C—C): 1.515, r(C—C): 1.540, r(C—H): 1.095, r(=C—H): 1.09

bond angle, Θ/°

Θ(C=C—C): 125, Θ(C=C—H): 120, other valence angles: tetrahedral.

[a] The units of the Urey–Bradley–Shimanouchi force constants are mdyn Å^{-1} for stretching (K), bending (H), repulsion (F), *cis* repulsion (R) and bond interaction (P), and mdyn Å for out-of-plane wagging (W), torsion (Y), the interaction constant (WW) between the two neighbouring CH wagging modes, the interaction constant (WY) between the CH wagging and C=C torsional modes, and *trans* and *gauche* interactions (TC and GC).

Results and Discussion

In our previous paper[15] we reported the vibrational spectra of two simple surfactants, potassium 4-pentenoate (P4P) and potassium 5-hexenoate (P5H), and discussed the conformation of these molecules. From the vibrational spectra and the predictions of normal-coordinate calculations, it was shown that the skew form about the C—C single bond adjoining the C=C double bond is stabilized at low temperatures. This conclusion has been directly confirmed by the use of the skeletal deformation region in the vibrational spectra.

In the present paper, for potassium *trans*-4-hexenoate (PT4H) the temperature dependence of the vibrational spectra in the 1700–100 cm^{-1} region were investigated and normal-coordinate calculations were also made in order to explain the vibrational spectra (table 2). Results similar to those for P4P and P5H were obtained, *i.e.* the TS and TC forms also coexist in crystalline PT4H at room temperature (300 K). The population of the TS form is much greater than that of the TC form at low temperature (100 K),

Table 2. Observed and calculated frequencies of PT4H[a]

obsd/cm^{-1}										
i.r.		Raman			calcd/cm^{-1}					
crystalline		aqueous	crystalline							
300 K	100 K	soln[b]	300 K	100 K	TS	TC	GS	G′S	GC	assignment[c]
695s	692s	711vw, b	700vw, b	691vw	699	707	—	—	—	sCO_2 (TS, TC)
—	—	660vw, b	—	—	—	—	677	680	679	sCO_2 (GS, G′S, GC)
—	—	620vw, b	—	—	—	—	—	—	605	wCO_2, δ=CCC (GC)
585vw, b	580w, b	583vw, b	585sh	580vw	583	582	582	586	—	wCO_2, $rC_\alpha H_2$ (TS, TC, GS, G′S)
575vw, b	—	—	573vw, b	—	—	564	—	—	574	$\delta C{=}CC_\beta$, $\delta{=}CCC_\alpha$ (TC), wCO_2, $rC_\alpha H_2$ (GC)
545m, b	548s	540vw, sh	546vw	550vw	535	—	541	535	—	rCO_2, $\delta{=}CCC_\alpha$ (TS, GS, G′S)
—	—	507vvw, sh	—	—	—	—	506	504	—	$\delta C_\omega C{=}C$, $\delta C{=}CC_\beta$ (GS, G′S)
489vw	(492vw)*	—	490vvw	(486sh)*	—	489	—	—	—	rCO_2, $\delta C_\omega C{=}C$ (TC)
467m	468s	479m	466m	467m	475	—	—	—	477	rCO_2, $\delta C_\omega C{=}C$ (TS, GC)
—	—	404vvw, b	—	—	—	—	375	376	367	rCO_2, $\delta{=}CCC_\alpha$ (GS), $\delta{=}CCC_\alpha$, $\delta C{=}CC_\beta$ (G′S), $\delta C_\omega C{=}C$, $\delta{=}CCC_\alpha$ (GC)
347vw	347w	353s	345s	347s	351	342	—	—	—	$\sigma C{=}CC_\beta$, $\delta{=}CCC_\alpha$ (TS), $\delta C_\omega C{=}C$, $\delta{=}CCC_\alpha$ (TC)
—	—	—	—	—	—	—	295	299	—	$\delta C_\omega C{=}C$, $\delta C{=}CC_\beta$ (GS, G′S)
281vw	284w	285vvw	279vvw	280vvw	284	—	—	—	279	$\delta C_\omega C{=}C$, $\delta C{=}CC_\beta$ (TS), $\tau CH_3{-}C$, $\tau C_\gamma{-}C_\beta$ (GC)
—	—	—	—	—	—	263	—	—	—	$\tau CH_3{-}C$, $\tau C_\gamma{-}C_\beta$ (TC)
246w, b	245w	—	244vw	244vvw, b	252	—	253	256	241	$\tau CH_3{-}C$ (TS, GS, G′S), $\tau CH_3{-}C$, o.p.=$C_\pi H$ (TC, GC)
—	—	—	—	—	—	231	—	—	231	$\tau CH_3{-}C$, o.p.=$C_\pi H$ (TC), $\delta C{=}CC_\beta$, $\delta CC{=}CC$ (GC)
—	185m, b	—	190vvw	200vvw, b	194	217	208	195	—	δCCC_α, $\tau C{=}C$ (TS), δCCC_α, $\delta C{=}CCC_\alpha$ (TC), δCCC_α, rCO_2 (GS, G′S)
166s, b	170w	—	—	165vvw, b	151	—	173	180	178	$\tau C_\gamma{-}C_\beta$, $\tau C_\beta{-}C_\alpha$ (TS), $\tau C{=}C$, o.p.=$C_\gamma H$ (GS, G′S), δCCC_α, $\tau C{=}C$ (GC)

—	—	1670vs	1674vs	1678vs	1671	1670	1671	1671	1670	νC=C, i.p.=C$_\pi$H (TS, TC, GS, G′S, GC)
1565vs	1565vs	1560vwb	1580m	1584m	1585	1585	1585	1585	1585	ν_aCO$_2$ (TS, TC, GS, G′S, GC)
—	—	1454m	1449msh	1450m	1451	1452	—	—	—	sC$_\alpha$H$_2$, sC$_\beta$H$_2$ (TS, TC)
1429sh, m	1434s	1443m	1434msh	1439m	—	—	1442	1443	1442	sC$_\alpha$H$_2$ (GS, G′S, GC)
—	—	—	—	—	1432	1432	1437	1437	1437	δaCH$_3$(A′) (TS, TC), sC$_\beta$H$_2$ (GS, G′S, GC)
—	—	—	—	—	1431	1431	1432	1432	1432	δaCH$_3$(A″) (TS, TC), δaCH$_3$ (A′) (GS, G′S, GC)
—	—	—	—	—	1426	1426	1431	1431	1431	sC$_\beta$H$_2$, sC$_\alpha$H$_2$ (TS, TC), δaCH$_3$ (A″) (GS, G′S, GC)
1415s	1418s	1415m	1420s	1422s	1422	1422	1421	1421	1421	ν_sCO$_2$, νC—CO$_2$ (TS, TC, GS, G′S, GC)
1383m	1381m	1380m	1385m	1379m	1385	1385	1385	1385	1385	ν_sCH$_3$, νCH$_3$—C (TS, TC, GS, G′S, GC)
—	—	—	—	—	—	1364	1360	1359	1362	wC$_\alpha$H$_2$, wC$_\beta$H$_2$ (TC, GS, G′S, GC)
1337w	1339w	1342w	1337w	1343w	1355	—	—	—	1338	wC$_\alpha$H$_2$, wC$_\beta$H$_2$ (TS), wC$_\alpha$H$_2$, i.p.=C$_\pi$H (GC)
1300w	1303w	1309s	1307s	1301s	1318	1325	1320	1317	—	i.p.CH=CH (TS, GS, G′S), i.p.=C$_\pi$H, wC$_\alpha$H$_2$ (TC)
—	1298w	—	—	—	1292	1288	1302	1305	1296	wC$_\beta$H$_2$, i.p.=C$_\gamma$H (TS, TC, GS, G′S), i.p.CH=CH (GC)
1270vvw	1273vw	1278m	1273m	1274m	1271	1268	1274	1273	1270	i.p.CH=CH (TS, TC, GS, G′S, GC)
1228w	1228m	1236w	1227w	1227w	1224	1225	1218	1219	—	tC$_\alpha$H$_2$ (TS, TC), tC$_\alpha$H$_2$, wC$_\beta$H$_2$ (GS, G′S, GC)
—	—	1209vw	—	—	—	1200	—	—	1214	tC$_\beta$H$_2$ (TC), tC$_\beta$H$_2$, wC$_\alpha$H$_2$ (GC)
1176vw	1176vw	1184w	1176w	1178w	1189	—	1183	1183	1192	tC$_\beta$H$_2$ (TS, GC), tC$_\beta$H$_2$, i.p.=C$_\pi$H (GS, G′S, GC)
1106vvw	1107vw	1108w	1110w	1109w	1109	1105	1105	1107	1103	νC$_\gamma$—C$_\beta$, νCH$_3$—C (TS, GS, G′S), νCH$_3$—C, rCH$_3$ (GC, TC)
1076vw	1076w	1073w	1076w	1078w	1078	1074	1078	1079	1079	νCH$_3$—C, νC$_\gamma$—C$_\beta$ (TS, TC, GS, G′S, GC)
1039vw	1036vvw	1040w	1040w	1042w	1039	—	1038	1039	—	νC$_\beta$—C$_\alpha$ (TS, GS, G′S)
(1025vw)	—	1020w	—	—	—	1019	—	—	1014	νC$_\beta$—C$_\alpha$, C—CO$_2$ (TC), νC$_\beta$—C$_\alpha$, rCH$_3$ (GC)
—	1012vw	—	—	—	1006	1005	1004	1004	1007	rCH$_3$, o.p.=C$_\pi$H (all isomers)
998vw	999w	—	999vw	999w	993	993	—	—	985	νC—CO$_2$, ν_sCO$_2$ (TS, TC), rC$_\beta$H$_2$, νC—CO$_2$ (GC)
—	—	977w	—	—	—	—	979	980	—	νC—CO$_2$, rC$_\beta$H$_2$ (GS, G′S)

Table 2. (*cont.*)

obsd/cm^{-1}										
i.r.		Raman								
crystalline		aqueous	crystalline		calcd/cm^{-1}					
300 K	100 K	soln[b]	300 K	100 K	TS	TC	GS	G′S	GC	assignment[c]
964m	968s	968w	965vw	961vw	972	966	—	—	—	$rC_\alpha H_2$, rCH_3 (TS), $rC_\alpha H_2$, $rC_\beta H_2$ (TC)
—	—	—	—	—	—	—	945	952	943	rCH_3, $rC_\alpha H_2$ (GS, G′S, GC)
930w	931w	940s	931s	932s	930	—	930	—	—	rCH_3, $rC_\alpha H_2$ (TS, GS)
—	—	—	—	—	—	921	—	905	906	rCH_3, $\nu C_\beta—C_\gamma$ (TC), $rC_\alpha H_2$, rCH_3 (G′S), rCH_3, $\nu C_\alpha—C_\beta$ (GC)
900w	900vw	885w	899vw	900vw	882	890	885	880	882	$\tau C=C$, o.p.$=C_\pi H$ (TS, TC), $\tau C=C$, o.p.$=C_\gamma H$ (GS, G′S, GC)
—	—	856w	—	—	—	—	—	861	855	$rC_\beta H_2$, o.p.$=C_\pi H$ (G′S), $rC_\beta H_2$, $rC_\alpha H_2$ (GC)
(830vw)	—	—	—	—	—	834	829	—	—	$rC_\beta H_2$, $rC_\alpha H_2$ (TC, GS)
800m	800w	804vw	801w	803w	813	—	—	—	—	$rC_\beta H_2$, $rC_\alpha H_2$ (TS)
—	—	—	—	—	—	—	768	762	—	o.p.$=C_\gamma H$, o.p.$=C_\pi H$ (GS, G′S)
753vw	756vw	762w, b	754w	755w	753	—	—	—	—	o.p.$=C_\pi H$, o.p.$=C_\gamma H$ (TS)
—	—	—	—	—	—	727	—	—	741	o.p.$=C_\gamma H$, $rC_\beta H_2$ (TC), o.p.$=C_\pi H$, o.p.$=C_\gamma H$ (GC)

[a] s, strong; m, medium; w, weak; v, very; sh, shoulder; b, broad. [b] Concentration of PT4H = 3.67 mol dm^{-3}. [c] s, scissoring; w, wagging; r, rocking; o.p., out-of-plane deformation; i.p., in-plane deformation; δ, deformation; τ, torsion; ν, stretching; ν_a, asymmetric stretching; ν_s, symmetric stretching. α, β, γ, π and ω denote the position of carbons of the PT4H skeleton ($C_\omega—C_\pi=C_\gamma—C_\beta—C_\alpha—CO_2^-$).

since the intensities of the TC bands are extremely weak in both the infrared and Raman spectra. Thus the TS form is preferentially stabilized on cooling to 100 K, compared to the TC form, in the crystal.

The vibrational spectra in the 1700–700 cm^{-1} region are sensitive to the molecular conformation, as has been shown in our previous papers.[14,15] Lippert and Peticolas[2] pointed out the utility of this region in conformation studies of unsaturated fatty acids. However, little is known about the detailed vibrational state of simple unsaturated surfactants by analysing the vibrational spectra and assignments due to normal-coordinate calculations. To carry out more detailed conformational studies, a normal-coordinate analysis of simple surfactants in this region is required. Our discussion is mainly devoted to the utility of vibrational spectra in the 1700–700 cm^{-1} region in conformation studies of PT4H.

The stabilization of the TS form caused by cooling affects the infrared spectrum in the 1700–700 cm^{-1} region. The infrared band at 831 cm^{-1} observed at 300 K decreases in intensity on cooling, and the band at 1025 cm^{-1} disappears at 100 K. The other infrared bands increase in intensity at low temperatures. The 831 and 1025 cm^{-1} bands are due to the TC form. The population of TC is very small at 100 K since the intensities of these vibrational bands are extremely weak. Assignment of these two bands to the TC form is supported by the calculated results of the normal-coordinate analysis (table 2); the observed wavenumbers of 1025 and 831 cm^{-1} closely correspond to the calculated ones, 1019 and 834 cm^{-1}, of the TC form. The wavenumbers of the other infrared bands and the corresponding Raman bands are in good agreement with the calculated ones of the TS form. Thus the vibrational bands of the crystalline PT4H in this region can be explained by the TS form, except for the above two bands.

For the vibrational modes characteristic of the —CH=CH— group, the out-of-plane deformation mode is particularly useful for conformation studies, because it is predicted from calculations that the wavenumber of this mode is dependent on the molecular conformation.

The vibrational modes characteristic of α- and β-CH_2 groups appear separately at the different wavenumbers, and are available for conformation studies.

Conformational Change on Micellization: Raman Scattering Studies

A change in conformation of simple surfactants on micelle formation in aqueous solution can be directly confirmed by measurements of the concentration dependence of the Raman spectrum in the 700–100 cm^{-1} region. For instance, in the case of simple surfactants having a saturated hydrocarbon chain, it has been found that the intensity of the Raman band due to an accordion-like vibration of the all-*trans* form of the chain rapidly increases on micellization.[6] This phenomenon is due to the predominant stabilization of the all-*trans* form in the micellar state. For simple surfactants having a C=C double bond, the stabilization of a specific rotational isomer on micellization has also been confirmed by the Raman spectra in the skeletal deformation region.[14,15]

In the present paper the Raman spectrum of PT4H in H_2O is dependent on concentration with regard to both the intensities and positions of the bands, as can be seen in fig. 1. The intensity of the 352–363 cm^{-1} band due to the TS form increases markedly with an increase in the concentration, while that of the 404 cm^{-1} band of the GS and G′S forms increases with dilution and broadening occurs [fig. 1(A)]. The ratio, $I_{352\text{-}363}/I_{404}$, increases rapidly with increasing concentration above 1.4–1.5 mol dm^{-3}, corresponding to the critical micelle concentration (c.m.c.).[29] This observation shows directly the preferential stabilization of the TS form on micellization. Moreover, at lower concentrations the 620–624 cm^{-1} band intensity is greater than that of the 660–665 cm^{-1} band, but it decreases at higher concentrations. This shows that the GC form is unstable at higher concentrations, compared to the GS and G′S forms.

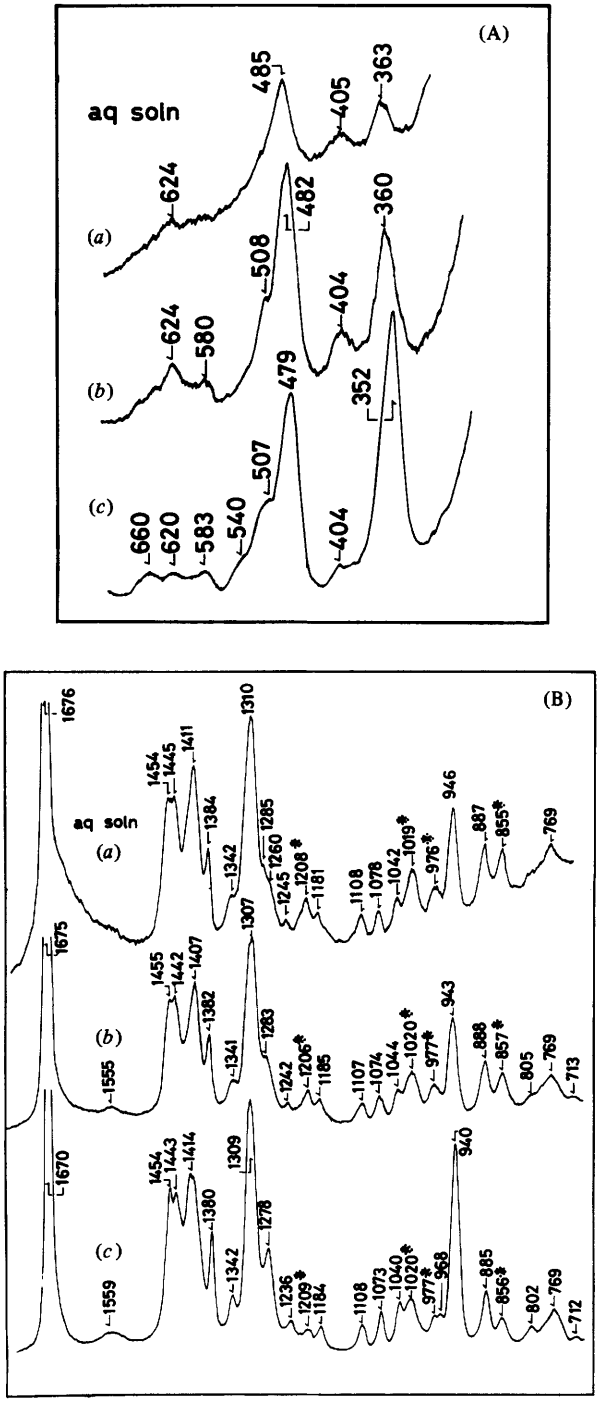

Fig. 1. Raman scattering spectra of PT4H–H_2O solutions [(*a*) 0.33, (*b*) 1.3 and (*c*) 4 mol dm^{-3}] in the 700–200 cm^{-1} region (A) and the 1700–700 cm^{-1} region (B) at room temperature.

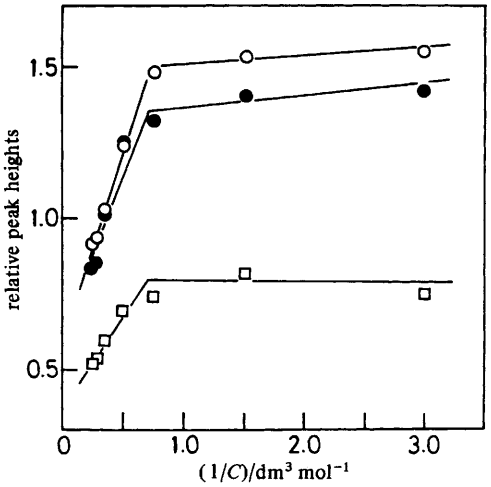

Fig. 2. Concentration dependence of the relative Raman peak heights (●, I_{1209}/I_{1189}; ○, I_{1020}/I_{1040} and □, I_{856}/I_{885}) in the 1700–700 cm^{-1} region.

Such a conformational change also brings about a shift in the wavenumber of the Raman bands. Those at 479 and 352 cm^{-1} in a 4 mol dm^{-3} aqueous solution are shifted to higher wavenumber as the concentration is lowered and reach 485 and 363 cm^{-1}, respectively, at a concentration of 0.33 mol dm^{-3}. The wavenumber shift also shows a stabilization of the other rotational isomers at low concentrations, except for the TS form.

The Raman spectrum in the region of 1700–700 cm^{-1} is sensitive to changes in conformation upon micellization. Fig. 1(B) shows the Raman spectra of a PT4H–H_2O solution at various concentrations. The Raman bands at 1454 and 1443 cm^{-1} are assigned to the scissoring modes of two methylene groups and the asymmetric deformation mode of the methyl group, respectively. From normal-coordinate analysis the 1454 cm^{-1} band is mainly due to the CH_2 scissoring of the TS and TC forms, and the 1443 cm^{-1} band also has a contribution from the CH_2 scissoring modes of other rotational isomers (GS, G′S and GC). The relative intensities of the two bands are dependent on the concentration. In the concentrated solutions (4 mol dm^{-3}) the intensity of the 1454 cm^{-1} band is larger than that of the 1443 cm^{-1} band. However, the 1443 cm^{-1} band increases in intensity with decreasing concentration. The intensity variation is due to the stabilization of TS or TC at higher concentrations.

In the 1330–1270 cm^{-1} region a broad and strong Raman band at 1309 cm^{-1} and a weak band at 1278 cm^{-1} are observed and are assigned to the in-plane deformation modes of the two =CH— groups. The intensity of the 1278 cm^{-1} band changes with concentration, as is seen in fig. 1(B). The intensity of the band decreases and its position is shifted as the sample solution is diluted. Accordingly, the in-plane deformation mode is also sensitive to a change in conformation.

Four Raman bands at 1209, 1020, 977 and 856 cm^{-1} observed in aqueous solution disappear in the crystalline state. From the normal-coordinate analysis assignments of these Raman bands were made as follows. The 1209 cm^{-1} band is assigned to the twisting mode of the $C_\beta H_2$ group adjacent to the C=C double bond of the TC and GC forms or that of the $C_\alpha H_2$ group of the GC form. The 1020 cm^{-1} band arises from the symmetric stretching vibration of the C_α—C_β bond of the TC and GC forms. The band at 977 cm^{-1} is due to the rotational isomers, except for the TS and TC forms, and is assigned to the coupled vibrational mode between the C—CO_2^- stretching and $C_\beta H_2$

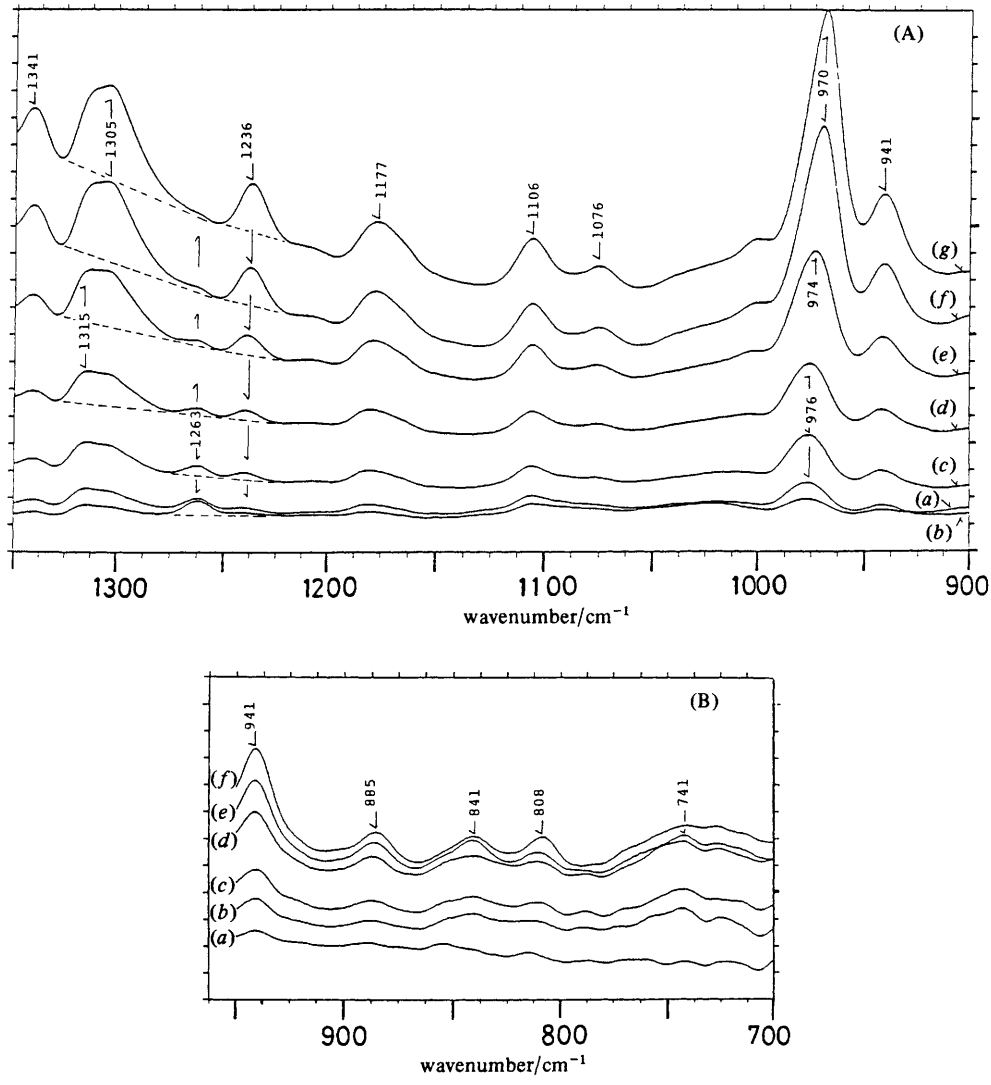

Fig. 3. The difference F.t.i.r. spectra of (A) PT4H–H_2O [(*a*) 0.33, (*b*) 0.64, (*c*) 0.99, (*d*) 1.32, (*e*) 1.97, (*f*) 2.63 and (*g*) 3.3 mol dm^{-3}] and (B) PT4H–D_2O [(*a*) 0.33, (*b*) 0.66, (*c*) 0.99, (*d*) 1.32, (*e*) 1.97 and (*f*) 2.63 mol dm^{-3}].

rocking modes, and the 856 cm^{-1} band corresponds to the rocking vibration of the $C_\beta H_2$ group of the G′S and GC forms.

The relative peak heights, I_{1209}/I_{1184}, I_{1020}/I_{1040} and I_{856}/I_{885}, decrease markedly with increasing concentration, as is seen in fig. 2. A point of inflection in the plots of the relative heights *vs.* the inverse concentration corresponds to the critical micelle concentration of the PT4H ions. The existence of such an inflection shows that a conformational change occurs upon micelle formation.

In the region of 800–700 cm^{-1}, a very weak, broad Raman band at 769 cm^{-1} and an extremely weak band at 710–715 cm^{-1} are observed, and are assigned to the out-of-plane deformation of the =CH— groups. The broadness of the 769 cm^{-1} band implies an overlapping of some bands, and it is difficult to discuss conformational changes using the

Raman bands in this region. However, the difference F.t.i.r. spectrum of the sample solution in this region is available for a study of conformational changes, as is discussed later.

F.T.I.R. Absorption Studies

The difference F.t.i.r. absorption spectra were measured for the aqueous solutions of PT4H. In the region 1500–900 cm^{-1} the infrared absorption spectrum of the H_2O molecule was successfully cancelled out.

Fig. 3(A) and (B) show the difference F.t.i.r. spectra of PT4H–H_2O (or PT4H–D_2O) solutions at various concentrations. For concentrated solutions (3.3 mol dm^{-3}) the infrared band at 1236 cm^{-1} corresponded to the 1230 cm^{-1} bands in crystalline PT4H arising from the $C_\alpha H_2$ twisting vibrational mode of the TS form. The absorbance of the 1236 cm^{-1} band increases markedly with an increase in the concentration. At low concentrations a new band at 1263 cm^{-1} appears owing to the in-plane deformation mode of the two =CH— groups of the rotational isomers, except the TS form. The absorbance of the 1263 cm^{-1} band decreases rapidly with an increase in concentration, and finally this band becomes a very weak shoulder at a concentration of 3.3 mol dm^{-3}. These observations reveal that the TS form is preferentially stabilized in higher concentration.

The absorbance of these two bands is plotted as a function of the reciprocal of the concentration in fig. 4. The absorbances of the 1236 and 1263 cm^{-1} bands change rapidly at a concentration of 1.4–1.5 mol dm^{-3}, and the curves do not follow the Beer–Lambert law. The inflections closely correspond to those in the plots of relative peak heights *vs.* $1/C$ of the Raman spectra discussed in the present paper. The variation in absorbance is due to micelle formation.

The infrared absorption bands at 1315 and 1305 cm^{-1} are assigned to the coupled bands of the in-plane deformation modes of the two =CH— groups and the wagging vibration of the $C_\beta H_2$ methylene group coupled with the in-plane deformation of the $=C_\gamma H—$ group, respectively. For these two bands a dependence on concentration of the absorbance is also found.

Dilution of the PT4H–H_2O solution results in an increase in the absorbance of the broad infrared band at 1020 cm^{-1}. This observation corresponds to the concentration dependence of the Raman band intensity at 1020 cm^{-1} (fig. 1 and 2).

The position of the infrared band at 970 cm^{-1} is dependent on concentration, as is seen in fig. 3(A). The wavenumber shift is also caused by the preferential stabilization of the TS form.

When D_2O was used as a solvent, the infrared absorption spectra of D_2O in the region 100–700 cm^{-1} were successfully cancelled out. The difference F.t.i.r. absorption spectra of PT4H in D_2O are found to be sensitive to changes in conformation, as is seen in fig. 3(B). The coupled modes of the rocking vibrations of the α- and β-methylene groups appear in the region 870–800 cm^{-1}. The infrared band at 808 cm^{-1}, corresponding to the Raman band at 804 cm^{-1}, is due to the rocking vibrational modes of the two methylene groups of the TS form, and the 841 cm^{-1} band is due to those of the TC and GS forms. The Raman band at 856 cm^{-1} arises from the G′S and GC forms.

In fig. 3(B) the absorbance of the 808 cm^{-1} band increases with increasing concentration, compared to that of the 841 cm^{-1} band. Such a variation occurs at concentrations near to the c.m.c. The infrared band at 855 cm^{-1} decreases in intensity with increasing concentration. This closely corresponds to the concentration dependence of the relative peak heights, I_{856}/I_{885}, in the Raman spectra of PT4H–H_2O solutions discussed above.

For the region 800–700 cm^{-1} the five bands at 770, 756, 743, 725 and 715 cm^{-1}, assigned to the out-of-plane deformation modes of the two —CH= groups for the five

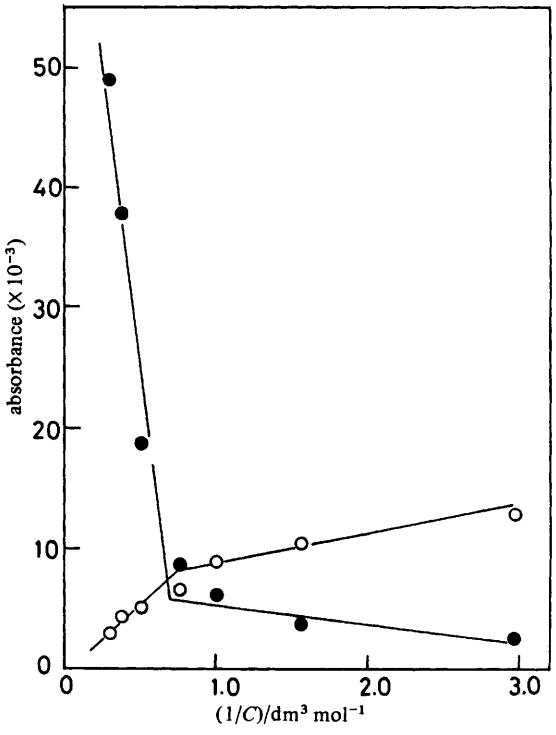

Fig. 4. Concentration dependence of the infrared band intensity in the difference F.t.i.r. spectra of PT4H–H_2O solutions (○, 1263 and ●, 1236 cm^{-1}).

rotational isomers, are due to the GS, G′S, TS, GC and TC forms, respectively. The intensities of these bands seems to be dependent on concentration. The 743 cm^{-1} band arising from the TS form increases in intensity with increasing concentration. The infrared bands at 788 and 770 cm^{-1} become a very weak shoulder in higher concentration, showing the instability of the GS and G′S forms in the micellar state.

Conclusions

Normal-coordinate analysis successfully explains the vibrational spectra of PT4H in the crystalline state and in aqueous solutions. In crystalline PT4H the TS and TC forms coexist at room temperature. However, the TS form is preferentially stabilized at lower temperatures.

In the micellar state of PT4H, the TS form is preferentially stabilized, compared to other rotational isomers. The stabilization of such a specific isomer causes an intensity change and wavenumber shift for a wide range of Raman spectra of aqueous solutions.

The difference F.t.i.r. spectra of PT4H–H_2O (or PT4H–D_2O) solutions are also available for the investigation of conformational changes. At a PT4H concentration > 0.3 mol dm^{-3} the difference F.t.i.r. spectra of H_2O or D_2O are successfully cancelled out, and reproducible difference F.t.i.r. spectra are obtained. For simple surfactants having a higher c.m.c., the change in intensity of infrared bands below and above the c.m.c. can be easily observed. Moreover, the wavenumber shift accompanying conformational change can also be measured precisely.

We express our gratitude to the Toyoda Physical and Chemical Research Institute for financial support.

References

1 J. L. Lippert and W. L. Peticolas, *Proc. Natl Acad. Sci. USA*, 1971, **68**, 1572.
2 J. L. Lippert and W. L. Peticolas, *Biochim. Biophys. Acta*, 1972, **282**, 8.
3 R. Mendelsohn, S. Sunder and H. J. Bernstein, *Biochim. Biophys. Acta*, 1975, **413**, 329.
4 S. P. Verma and D. F. Wallach, *Biochim. Biophys. Acta*, 1976, **436**, 307.
5 H. Okabayashi, M. Okuyama, T. Kitagawa and T. Miyazawa, *Bull. Chem. Soc. Jpn*, 1974, **47**, 1075.
6 H. Okabayashi, M. Okuyama and T. Kitagawa, *Bull. Chem. Soc. Jpn*, 1975, **48**, 2264.
7 A. Seelig and J. Seelig, *Biochemistry*, 1977, **16**, 45.
8 P. J. Davis, B. D. Fleming, K. P. Coolbear and K. M. W. Keough, *Biochemistry*, 1981, **20**, 3633.
9 K. P. Coolbear, C. B. Berde and K. M. W. Keough, *Biochemistry*, 1983, **22**, 1466.
10 B. P. Graber and W. L. Peticolas, *Biochim. Biophys. Acta*, 1977, **465**, 260.
11 R. C. Lord and R. Mendelsohn, in *Membrane Spectroscopy*, ed. E. Grell (Springer, New York, 1981), pp. 377–426.
12 S. K. Hark and J. T. Ho, *Biochim. Biophys. Acta*, 1980, **601**, 54.
13 N. R. Chen and J. T. Ho, *Biochem. Biophys. Res. Commun.*, 1985, **127**, 220.
14 H. Okabayashi and M. Abe, *J. Phys. Chem.*, 1980, **84**, 999.
15 K. Tsukamoto, K. Ohshima, K. Taga, H. Okabayashi and H. Matsuura, *J. Chem. Soc., Faraday Trans. 1*, 1987, **83**, 789.
16 J. Umemura, H. H. Mantsch and D. G. Cameron, *J. Colloid Interface Sci.*, 1981, **83**, 558.
17 T. Kawai, J. Umemura and T. Takenaka, *Colloid Polym. Sci.*, 1984, **262**, 61.
18 D. G. Cameron, H. L. Casal, E. F. Gudgin and H. H. Mantsch, *Biochim. Biophys. Acta*, 1980, **596**, 463.
19 D. G. Cameron, E. Gudgin and H. H. Mantsch, *Biochemistry*, 1981, **20**, 4496.
20 R. A. Dluhy, R. Mendelsohn, H. L. Casal and H. H. Mantsch, *Biochemistry*, 1983, **22**, 1170.
21 R. A. Dluhy, D. G. Cameron, H. H. Mantsch and R. Mendelsohn, *Biochemistry*, 1983, **22**, 6318.
22 R. A. Dluhy, B. Z. Chowdhry and D. G. Cameron, *Biochim. Biophys. Acta*, 1985, **821**, 437.
23 R. A. Dluhy, D. Moffatt, D. G. Cameron, R. Mendelsohn and H. H. Mantsch, *Can. J. Chem.*, 1985, **63**, 1925.
24 J. Umemura, M. Matsumoto, T. Kawai and T. Takenaka, *Can. J. Chem.*, 1985, **63**, 1713.
25 E. N. Eccot and R. P. Linstead, *J. Chem. Soc.*, 1929, 2163.
26 Y. Koyama and K. Ikeda, *Chem. Phys. Lipids*, 1980, **84**, 999.
27 S. Abrahamson and I. Ryderstedt-Nahringbauer, *Acta Crystallogr.*, 1961, **15**, 1261.
28 T. Shimanouchi, *Computer Program for Normal Coordinate Treatment of Polyatomic Molecules* (University of Tokyo, 1968).
29 H. Okabayashi, M. Okuyama and T. Kitagawa, *Bull. Chem. Soc. Jpn*, 1975, **48**, 2264.

Paper 7/1168; *Received* 29*th June*, 1987